Available online at www.sciencedirect.com
ScienceDirect
Polymer 48 (2007) 5850–5858
polymer
www.elsevier.com/locate/polymer

Synthesis of TiO_2/PAA nanocomposite by RAFT polymerization

Behnaz Hojjati, Ruohong Sui, Paul A. Charpentier*

Department of Chemical and Biochemical Engineering, University of Western Ontario, London, Ontario, Canada N6A-5B1

Received 12 May 2007; received in revised form 15 July 2007; accepted 21 July 2007
Available online 29 July 2007

Abstract

Due to the strong tendency of nanoparticles such as metal oxides to agglomerate, homogeneous dispersion of these materials in a polymeric matrix is extremely challenging. In order to overcome this problem and to enhance the filler–polymer interaction, this study focused on living polymerization that was initialized from the surface of titania nanofillers. A new method for synthesizing TiO_2/polymer nanocomposites was found with a good dispersion of the nanofillers by using the bifunctional RAFT agent, 2-{[(butylsulfanyl)carbonothioyl]sulfanyl}propanoic acid). This RAFT agent has an available carboxyl group to anchor onto TiO_2 nanoparticles, and an S=C(SC_4H_9) moiety for subsequent RAFT polymerization of acrylic acid (AA) to form n-TiO_2/PAA nanocomposites. The functionalization of n-TiO_2 was determined by FTIR and partitioning studies, the livingness of the polymerization was verified using GPC and NMR, while the dispersion of the inorganic filler in the polymer was studied using electron microscopy, FTIR and thermal analysis.

Keywords: TiO_2; Polyacrylic acid; Nanocomposite

1. Introduction

In the last decade, the synthesis of polymer nanocomposite materials has been intensely studied due to their extraordinary properties and wide-spread potential applications. As the matrices of nanocomposites, a wide variety of polymers have been explored, while a diversity of crystalline materials, i.e., three-dimensional nano metal oxides [1,2], two-dimensional layered silicates such as nanoclays [3], and one-dimensional carbon nanotubes [4] have been used for reinforcement of the polymer matrices [5]. Recently, attention to the nanoscale metal oxides has grown due to their unique properties, low cost, and multiple potential applications [6,7]. Among these, nanotitania (n-TiO_2) is of significant scientific and industrial interest for several applications, such as a dye in conjugated polymers for photoelectrochemical [8] or photoconductive agents [9], a photocatalyst in a photodegradable TiO_2/polystyrene nanocomposite films [10], and semiconductor electrodes in photoelectrochemical cells [11]. Especially, TiO_2/polyelectrolyte composites such as TiO_2/poly(ethyleneimine)/poly(acrylic acid) (PAA) are materials of interest for their potential application for the solid electrolytes in dye-sensitized solar cells [12].

Due to their extremely large surface-area/particle-size ratio, nanoparticles tend to strongly agglomerate, hence reducing the resultant mechanical properties of the nanocomposite materials [13]. Many efforts have been taken in order to overcome this problem and to enhance the filler–matrix interaction. One approach is breaking down the agglomerated nanoparticles using a mechanical method such as ultrasonic irradiation, which has been explored for dispersion of SiO_2, TiO_2, and Al_2O_3 nanoparticles during the synthesis of inorganic/polymer nanocomposite materials [14–16]. However, this approach is restricted due to the limited interaction between the inorganic fillers and the organic matrix, compared with the very strong interaction between individual nanoparticles. An improved approach is modifying the surface of the inorganic filler and covalent attachment to polymer chains to minimize agglomeration and to strengthen the interaction between the nanofiller and polymer matrix, as illustrated schematically in Fig. 1

* Corresponding author. Tel.: +1 519 661 3466; fax: +1 519 661 3498.
E-mail address: pcharpentier@eng.uwo.ca (P.A. Charpentier).

0032-3861/$ - see front matter © 2007 Elsevier Ltd. All rights reserved.
doi:10.1016/j.polymer.2007.07.054

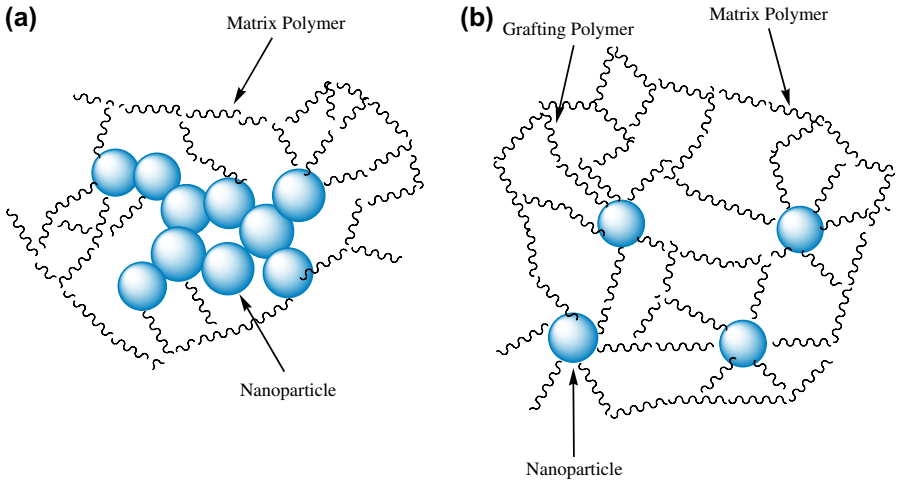

Fig. 1. Schematics of: (a) agglomerated nanoparticles in the matrix polymer in the case without grafting polymer and (b) separation of particles due to the grafting polymer [18,19].

[17,18]. Using the ''grafting to'' approach, the number of polymer chains that one can graft to the nanosurface is generally small, as the free volume occupied by each grafted polymer chain acts as a barrier to the attachment of subsequent polymer chains. Hence, ''grafting to'' is increasingly difficult as more chains are added to the surface, limiting control of the molecular weight and polydispersity of the polymer chains. On the other hand, using ''grafting from'' with initiators initially anchored to the nanosurface allows monomer molecules to easily diffuse to the surface of the particles, allowing higher graft density and better control of molecular weight and polydispersity of the polymer chains [19–21].

Various polymers such PS, PMMA, and PnBuA have been successfully ''grafted from'' nanoparticles via living/controlled radical polymerization techniques [22–27]. Ejaz et al. [28] grew polymer chains of methyl methacrylate from solid surfaces including silicon wafers, silica particles, and glass filters, by applying atom transfer radical polymerization (ATRP). Kong et al. [29] functionalized multiwalled carbon nanotubes by ATRP polymerization of styrene.

Using the relatively new technique of reversible addition-fragmentation chain-transfer (RAFT) polymerization, which has several advantages including polymerizing acidic monomers such as acrylic acid (AA), Baum and Brittain [30] polymerized St and MMA from silica nanoparticles, while Cui et al. [31] polymerized St successfully from multiwalled carbon nanotubes. RAFT confers living/controlled character to the polymerization with a mechanism suggested by Vana et al. [32] (Scheme 1) which includes: (I) initiation, (II) pre-equilibrium involving the initial RAFT chain-transfer agent

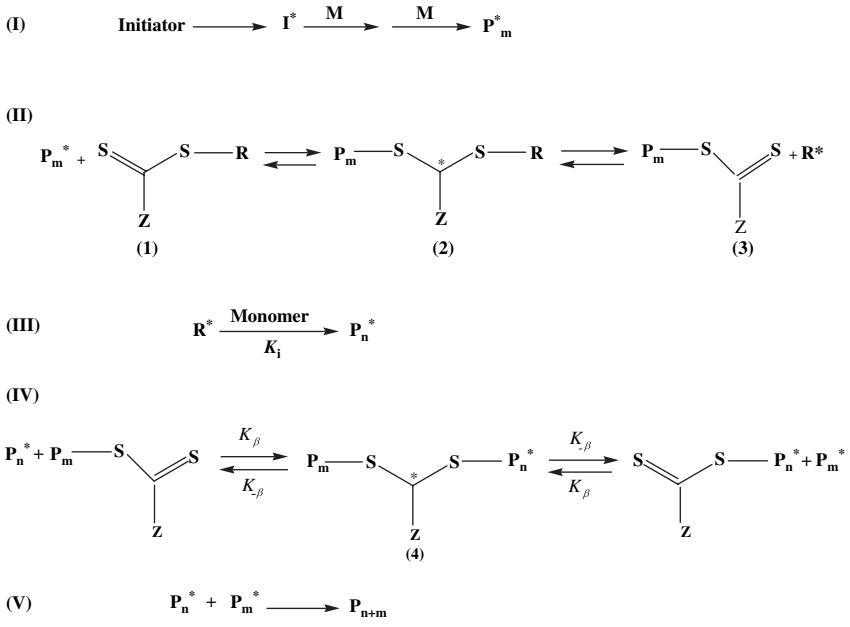

Scheme 1. Mechanism of RAFT polymerization [32].

(CTA), (III) propagation and re-initiation, (IV) chain equilibration (the core of RAFT polymerization), and (V) termination.

The key factor that makes RAFT a living polymerization technique is the choice of the RAFT agent. This choice depends on the monomer structure, leaving group R, and group Z in RSC (Z) = S [32]. In this study, two kinds of RAFT agents (**1** and **2** in Scheme 2) were synthesized to determine which one is appropriate for the acrylic acid monomer. Then ''grafting from'' polymerization with nanotitania (n-TiO_2) was attempted using the RAFT technique. Anchoring of the RAFT agent to the surface can be accomplished via either the Z or R group; however, most studies have chosen the R group [21], which leads to a scenario more closely resembling ''grafting from''. The mechanism of attachment of the Z group to the nanoparticles' surface is similar to that of ''grafting to'', with the intrinsic difficulties described above.

Our approach in selecting the RAFT initiator agent was to choose a R structure with a free carboxylate group that can coordinate to Ti(VI) on the titania surface. Rotzinger et al. [33] explored the attachment of a carboxylic group to a TiO_2 surface as sensitizers in dye-sensitized solar cells, and identified three possible coordination modes, monodentate, chelating or bridging bidentate (Scheme 3). Using this approach, we previously reacted the bifunctional molecule, methacrylic acid, to coordinate to n-TiO_2 with subsequent free-radical polymerization of methyl methacrylate to form the nanocomposite n-TiO_2/PMMA [34]. This research explored a living technique using the bifunctional RAFT agent, 2-{[(butylsulfanyl)carbonothioyl]sulfanyl}propanoic acid) (**1**). RAFT agent **1** was used to coordinate to n-TiO_2, while the S=C(SC_4H_9) moiety was used for subsequent RAFT polymerization of acrylic acid (AA), as illustrated schematically in Fig. 2. Coordination of the RAFT agent onto the n-TiO_2 was confirmed using ATR-FTIR analysis, livingness of the solution polymerization of AA was demonstrated by solution polymerization using **1** with subsequent ^{1}H NMR and GPC analysis, while the resulting nanocomposites were characterized by electron microscopy, FTIR, and thermal analysis.

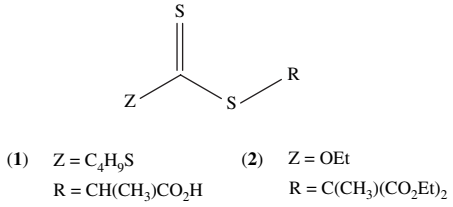

(**1**) Z = C_4H_9S, R = $CH(CH_3)CO_2H$ (**2**) Z = OEt, R = $C(CH_3)(CO_2Et)_2$

Scheme 2. Structures of RAFT agents (**1**) and (**2**).

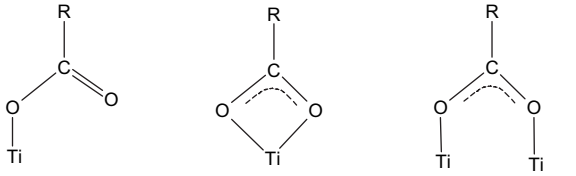

Scheme 3. Coordination modes of $RCOO^-$ with titania surface.

2. Experimental

2.1. Materials

Titania nanospherical particles (n-TiO_2) (99.5%, Sigma–Aldrich, avg. part. size 25–70 nm), 2,2′-azobis(2-methylpropionitrile) (AIBN) initiator (Toronto Research Company), methanol (HPLC grade, Sigma–Aldrich), hydrochloric acid (39%, Sigma–Aldrich), and radical inhibitor BHT (2,6-di-*tert*-butyl-4-methylphenol, 99%, Sigma) were used as received. Acrylic acid (AA) monomer (99%, Sigma–Aldrich, inhibited with 200 ppm BHT) was passed through an inhibitor remover column (Sigma–Aldrich) before use. The RAFT agents (2-{[(butylsulfanyl)carbonothioyl]sulfanyl}propanoic acid) (**1**) and 2-((ethoxythiocarbonyl)-2-methyl malonate (**2**) (Scheme 2) were prepared as described elsewhere [35].

2.2. RAFT polymerization of acrylic acid

A 0.0229 mol/L solution of RAFT agent (**1/2**) and a 2.29 mol/L solution of acrylic acid ([AA]/[RAFT agent] = 100) were dissolved in 150 ml methanol in a 250 ml three-neck flask equipped by a line of nitrogen supply, a thermometer, a stirrer for gentle mixing, and a condenser (with silica gel at the top for moisture removing). The solution was first heated to 65 °C, then 0.00229 mol/L of AIBN was added, which acted as an initiator ([RAFT agent]/[AIBN] = 10). At various times during the polymerization, GPC samples were

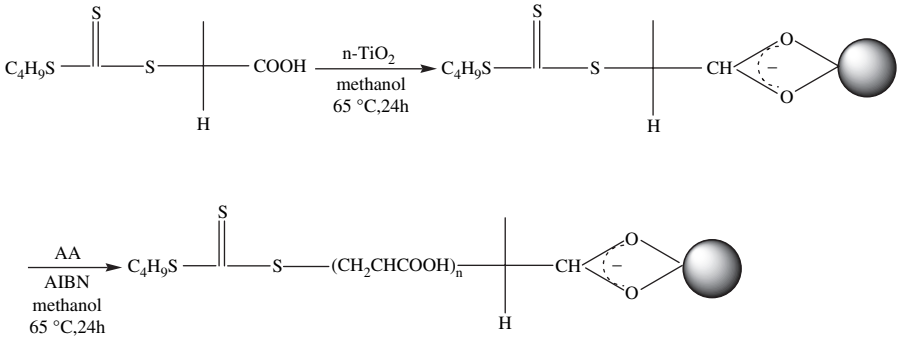

Fig. 2. Functionalization of TiO_2 and formation of PAA–TiO_2 nanocomposite.

prepared by removing small samples of the reaction mixture, inhibiting polymerization by BHT as radical inhibitor, solvent stripping in vacuum at 40 °C, and then re-dissolving in an aqueous buffer ($NaHCO_3$ 0.05 M, $NaNO_3$ 0.1 M, NaN_3 0.02 M) before molecular weight analysis.

2.3. Functionalization of n-TiO_2

RAFT agent (**1**) of 4.5 g and 1.5 g of n-TiO_2 were dispersed in 50 ml methanol with the aid of ultrasound for 1 h. The dispersed solution was then transferred to a 100 ml round bottom flask equipped with a condenser and a magnetic stirrer under nitrogen. The solution temperature was maintained at 65 °C under stirring for 24 h. After filtering the reaction product through a 0.05 μm polycarbonate membrane filter, the unreacted RAFT agent was removed by washing with methanol, and the solid product was dried overnight under vacuum at 60 °C.

2.4. Acrylic acid graft polymerization from RAFT agent anchored from n-TiO_2

Acrylic acid monomer of 0.6 g, 0.06 g of functionalized TiO_2–RAFT agent (10:1 wt/wt), and 0.004 g of AIBN were dispersed in 60 ml methanol with the aid of ultrasonication. Then the solution was transferred to a 100 ml three-neck flask equipped with nitrogen supply, a thermometer, and a condenser under constant stirring for 24 h. The mixture was diluted with methanol and filtered through a 0.05 μm polycarbonate membrane filter. To ensure that any ungrafted polymer was removed from the product, the filtered solid product was rinsed with methanol several times. The resulting solid product was then dried overnight under vacuum at 60 °C.

2.5. Cleaving grafted polymer from particles

PAA of 30 mg "grafted from" TiO_2 nanoparticles was dissolved in 1 ml of HCL (2 M) and 30 ml of deionized water. The solution was allowed to stir at 80 °C under reflux overnight. After filtration through a 0.05 μm polycarbonate membrane filter, the solution was poured into a glass plate and allowed to stand in a fume hood overnight. The recovered PAA was dissolved in an aqueous buffer ($NaHCO_3$ 0.05 M, $NaNO_3$ 0.1 M, NaN_3 0.02 M) for subsequent GPC analysis.

3. Characterization

The molecular weight and PDI of PAA were measured by gel permeation chromatography (GPC) with an Agilent 1200 using a RI detector referenced to PEO standards (1 ml/min, at 30 °C). ^{1}H NMR spectroscopy was operated on a Varian Mercury 400 while FTIR spectra were collected using a KBr pellet on a Bruker IFS 55 FTIR instrument attached with a MCT detector, with a resolution of 2 cm^{-1} and 128 scans for each sample. Scanning electron microscopy (SEM) images and energy dispersive spectrometer (EDS) were recorded using a Hitachi S-2600N without gold coating at 10 kV, transmission electron microscopy (TEM) was performed on a Phillips CM 10 electron microscope at 80 kV, and STEM was performed using a Hitachi HD2000 at 200 kV. Thermo gravimetric analysis (TGA) was performed using a TGA Q500 at a heating rate of 10 °C/min under nitrogen.

4. Results and discussion

4.1. RAFT polymerization of AA

4.1.1. ^{1}H NMR

As described in the introduction, RAFT polymerization achieves living growth starting from the initial dithioester or trithiocarbonate RAFT agent, which is activated by radicals generated from a traditional initiator [36] e.g. AIBN in this case. The synthesized RAFT agent (**1**) and PAA in methanol-d_4 were examined using ^{1}H NMR (Fig. 3). In Fig. 3a, the peaks B, C and E–H are assigned to the RAFT agent [37], and peaks I and J in Fig. 3b are attributed to the repeating unit of PAA [38]. Peak A is due to CD_3OH that is generated through substitution of methanol-d_4 and carboxylic acid, and peak D is from the solvent. The NMR spectrum in Fig. 3b shows that the functional groups of the RAFT agent are retained in the polymer, which provides strong evidence for the RAFT reaction occurring.

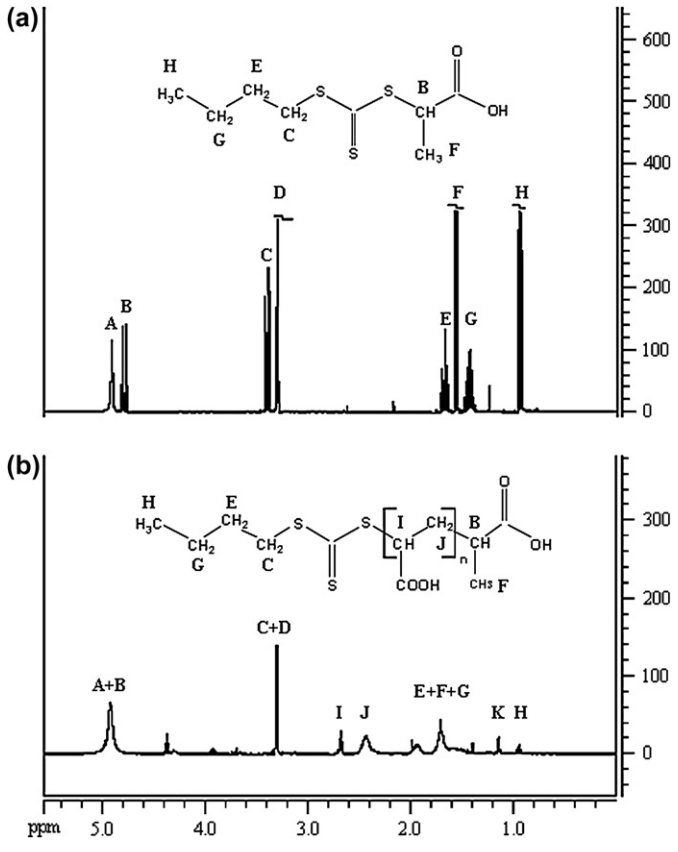

Fig. 3. ^{1}H NMR spectra of (a) 2-{[(butylsulfanyl)carbonothioyl]sulfanyl}-propanoic acid (**1**), and (b) PAA.

4.1.2. Molecular weight determination

Living polymerization is characterized by a linear increase of the molecular weight with conversion and reaction time, and a very narrow molecular weight distribution as evidenced by a polydispersity index (PDI = M_w/M_n) approaching 1. Table 1 shows the M_n values of acrylic acid synthesized by using two kinds of RAFT agents (**1** and **2** in Scheme 2) at different concentration ratios (mol/L). By using **2**, after 1 h the M_n of the polymer is relatively unchanged with polymerization time and the PDIs are broad, which is in contrast with the data obtained by Ladaviere et al. [39], where the M_n increased with time and the PDIs were narrow. As mentioned earlier, the effectiveness of the RAFT agent depends on both the monomer structure, and the R and Z groups. Moad et al. [40] showed that RAFT agents having O or N atoms (e.g. *O*-alkyl xanthate and *N*,*N*-dialkyl dithiocarbamate derivatives) are not very effective RAFT agents due to the interaction between O or N lone pairs and the C=S double bond, resulting in delocalization of this bond (Scheme 4). This helps to explain why RAFT agent **2** controlled the molecular weight poorly.

On the other hand, the molecular weights of polyacrylic acid synthesized by **1** increased linearly with time, and gave very narrow PDIs. As well, the polymer obtained with **2** was white, while that obtained from **1** had a yellow tinge, indicating the presence of the RAFT agent, which was also confirmed by the ^{1}H NMR results (above). Fig. 4 shows the GPC elution profiles of the PAA obtained using solution polymerization with RAFT agent **1**, where additional experiments were carried out for longer periods of time. The molecular weights of PAA increased directly with reaction time, and PDIs were in the range of 1.10–1.14. These results confirmed that the RAFT agent **1** was involved in a living polymerization reaction.

4.2. Nanoparticle functionalization and graft polymerization

4.2.1. FTIR study

In order to verify the functionalization of n-TiO_2 as well as the formation of the nanocomposite, FTIR analysis was carried out as FTIR is an established technique for analyzing the complexes of metal carboxylate species [41–44]. The spectrum of the RAFT agent (**1**) in Fig. 5a exhibits peaks at

Table 1
Polymerization of AA at different [AA]/[RAFT agent] in methanol as a solvent, at 65 °C, and AIBN as an initiator, [RAFT agent]/[AIBN] = 10, [AA] = 2.29 mol/L

Time (h)	**1**				**2**			
	[AA]/[**1**]				[AA]/[**2**]			
	50		100		50		100	
	M_n	PDI	M_n	PDI	M_n	PDI	M_n	PDI
1	1700	1.12	3600	1.11	6000	1.82	6500	1.79
2	2900	1.10	4700	1.10	5600	1.68	6300	1.76
3	3200	1.07	6300	1.06	5000	2.18	6100	1.87

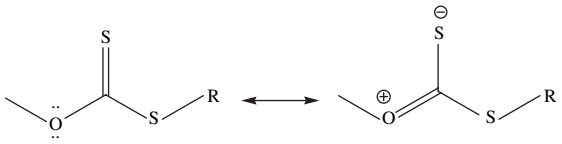

Scheme 4. Canonical form of xanthates and dithiocarbamates [40].

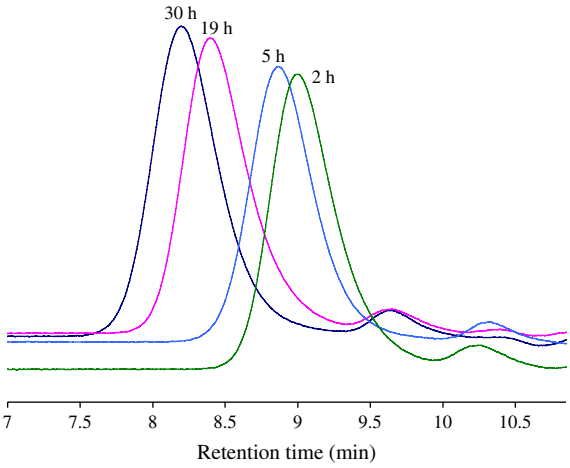

Fig. 4. GPC elution profiles for RAFT polymerization of acrylic acid using RAFT agent **1** at 65 °C, for 2 h (M_n = 2900 g/mol, PDI = 1.10), 5 h (M_n = 3980 g/mol, PDI = 1.12), 19 h (M_n = 8000 g/mol, PDI = 1.13), 30 h (M_n = 10,000 g/mol, PDI = 1.14).

1707 cm^{-1} (carboxylic group), 1375–1450 cm^{-1} (alkane groups), and no obvious peak in the region from 1475 to 1650 cm^{-1}. The new peaks at 1547, 1568, and 1626 cm^{-1} of the functionalized n-TiO_2 are assigned to the bridging or chelating bidentate coordination between titanium atoms and the carboxyl groups (Fig. 5b). The small peaks at 1708 and 1746 cm^{-1} are attributed to residual un-coordinated RAFT agent and carboxylate monodentate, respectively. In the spectrum of a typical n-TiO_2/PAA composite, the strong peak at 1724 cm^{-1} shows the existence of the carboxylic group, and the broad peaks in the range of 1500–1625 cm^{-1} show the remaining Ti-acetate bidentate (Fig. 5c). The small peak at 1653 cm^{-1} indicates the presence of adsorbed water, which remained in the nanocomposite even after vacuum drying, due to the superadsorbent nature of PAA. The FTIR spectra confirm that the TiO_2 nanoparticles were successfully functionalized with the carboxylic group of the RAFT agent.

4.2.2. Organic/water partitioning study

In addition to FTIR, the resulting materials were studied by organic phase/water partitioning experiments. As one would expect after functionalization by an organic group, n-TiO_2's hydrophilicity changes. Fig. 6a shows the n-TiO_2 dispersed in ethyl acetate/water bilayers, where the n-TiO_2 is suspended in the water phase (lower phase), indicating that it is hydrophilic. The n-TiO_2 functionalized with the RAFT agent, however, partitions into the organic phase (upper), due to the existence of the organic moiety, mainly contributed by –Bu groups (Fig. 6b). Due to many carboxylic groups and a few

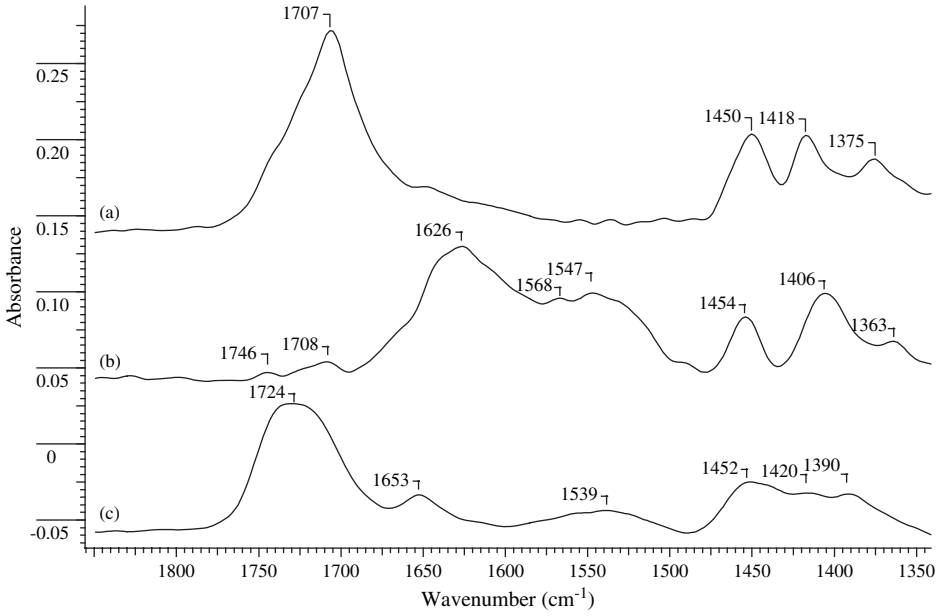

Fig. 5. FTIR spectra of (a) the RAFT agent **1**, (b) the functionalized n-TiO_2 and (c) the n-TiO_2/PAA composite.

–Bu groups in the PAA molecules, the n-TiO_2/PAA composite is mainly hydrophilic in nature, as evidenced by partitioning into the water phase (Fig. 6c).

4.3. Molecular weight determination of cleaved PAA

In order to determine whether the polymerization was still living when the RAFT agent had been coordinated to the n-TiO_2, the PAA was cleaved after various polymerization times using acidic conditions. The GPC results are presented in Table 2, which show that the number average molecular weight increased directly with reaction time, and the PDIs were relatively low. For the PAA/n-TiO_2 composites, thermo gravimetric analysis (TGA) showed an increase in PAA polymer content with increased polymerization time (Table 2). These results indicate that the anchored RAFT agent participated in the living polymerization of acrylic acid.

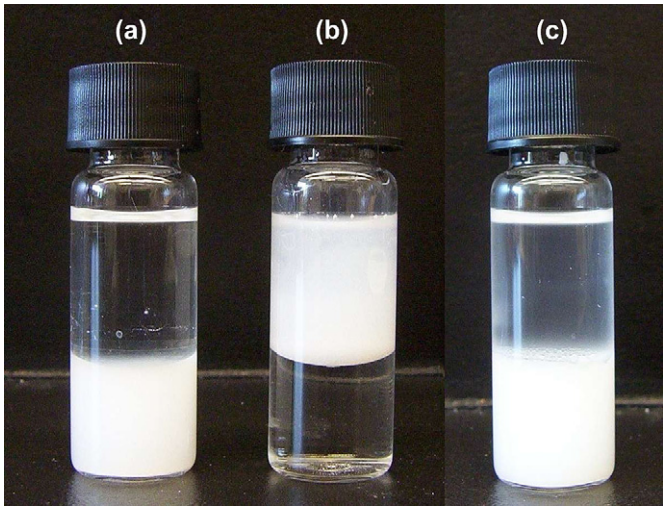

Fig. 6. In the vials, the upper layer is ethyl acetate and the lower layer is the water phase. The non-functionalized n-TiO_2 is well dispersed in the water phase (a), while the functionalized n-TiO_2 is suspended in the organic phase (b) and n-TiO_2/PAA composite stays in the water phase (c).

4.3.1. TGA analysis

The functionalized TiO_2, n-TiO_2/PAA nanocomposites, and cleaved TiO_2 were dried and subjected to TGA. As expected, the sample of crude TiO_2 gave no apparent weight loss below 700 °C (Fig. 7a). On the contrary, the sample of RAFT agent coordinated to n-TiO_2 displayed a weight loss of 4%, which was removed during heating in the range of 150–450 °C. Similarly for the n-TiO_2/PAA at different polymerization times (Fig. 7b), the weight loss occurred in the range of 150–450 °C. Higher fractions of PAA were formed as the polymerization time increased, indicating the successful graft polymerization of AA from the RAFT functionalized n-TiO_2. After cleaving under acidic conditions for 24 h (Fig. 7c), TGA analysis of the n-TiO_2 fraction showed 5% weight loss, indicating that almost 88% of the polymer chains were cleaved from the n-TiO_2 under the explored experimental conditions.

4.3.2. Electron microscopy

In order to examine the microstructure and nanofiller distribution within the polymer matrix, SEM equipped with EDS

Table 2
Molecular weight and PDIs (GPC) of cleaved PAA at different reaction times and fraction of grafted PAA (wt%) (TGA)

Time (h)	M_n (GPC) (g/mol)	PDI	Fraction of grafted PAA (TGA) (wt%)
6	5000	1.23	9
19	10,000	1.17	41.6
24	10,800	1.50	47.8

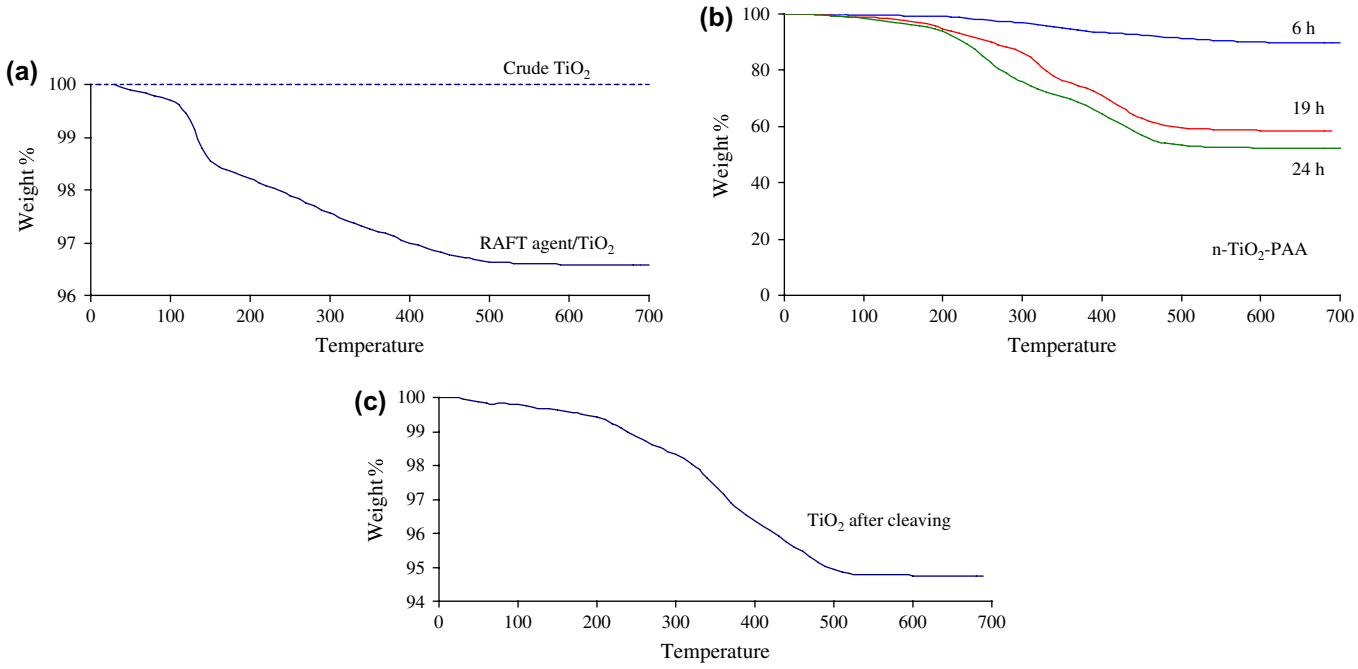

Fig. 7. TGA curves of the crude and functionalized TiO_2, n-TiO_2/PAA at different times, and TiO_2 after cleaving.

and TEM electron microscopy were used. SEM was used to study the morphology of n-TiO_2 before and after functionalization, as well as the polymer nanocomposites. Fig. 8a shows the SEM image of the commercial n-TiO_2 consisting of agglomerated spherical particles, whereas Fig. 8b shows the n-TiO_2 after functionalization. No obvious morphology change can be observed from the functionalization step. Fig. 8c shows the EDS sulfur mapping of RAFT functionalized n-TiO_2, showing well-distributed sulfur in the nanomaterials, indicating successful functionalization. Fig. 8d shows the n-TiO_2/PAA nanocomposite formed after ''grafting from'' polymerization with AA in which many nanoparticles with

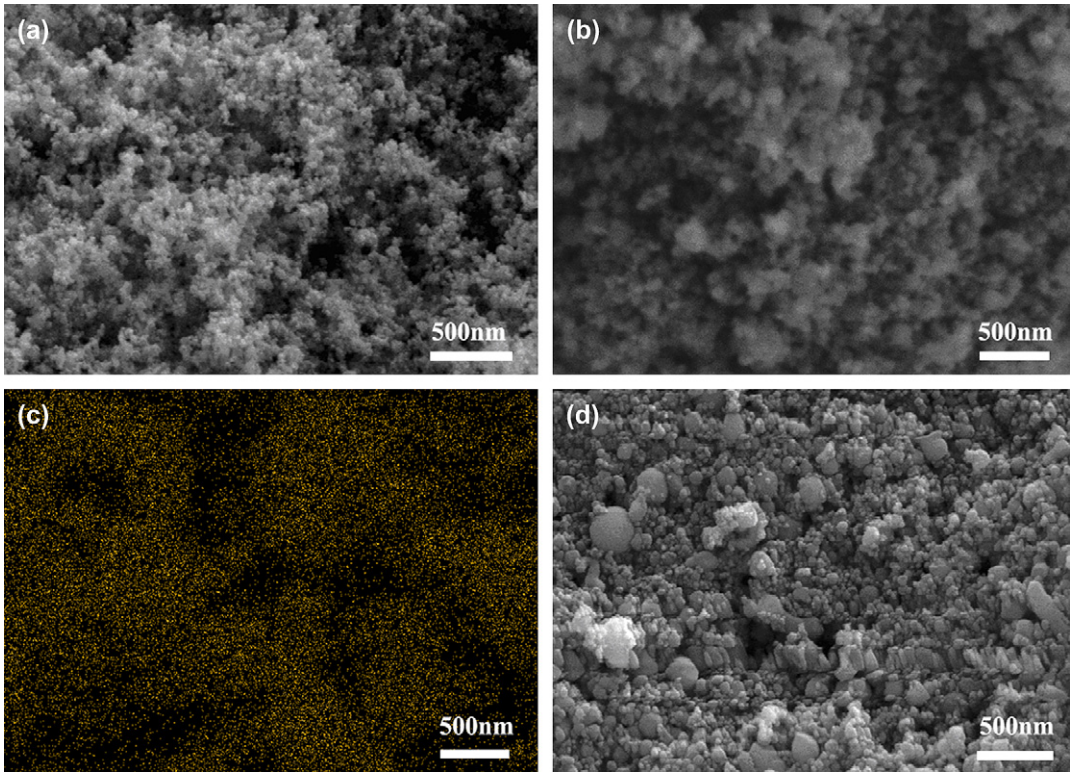

Fig. 8. SEM of the non-functionalized n-TiO_2 (a), SEM and EDS sulfur mapping of RAFT functionalized n-TiO_2 (b and c), and SEM of n-TiO_2/PAA composite (d).

a diameter of ca. 20–400 nm can be observed. These are attributed to the polymer chains that can only grow from the RAFT agent attached to the n-TiO_2 surface, resulting in the formation of n-TiO_2/PAA nanocomposite, which were also characterized by TGA (above).

The n-TiO_2/PAA composites were examined with TEM and STEM (Fig. 9a–d). Fig. 9a and b shows the well-dispersed n-TiO_2 at low magnification, while Fig. 9c shows the n-TiO_2 at higher magnification. Under high magnification using both bright and dark field electron microscopy, the ''grafting from'' polymer surrounding the n-TiO_2 can be clearly observed (Fig. 9d and e). Comparing with our former work on TiO_2/PMMA composites [34], the RAFT technique gave much better separation of the n-TiO_2 particles. The excellent separation of n-TiO_2 particles in this work is attributed to the growing of grafting AA polymer, which separates the previously agglomerated TiO_2 nanoparticles. In addition, as PAA is known as a polyelectrolyte, this may also contribute to the excellent dispersion of the TiO_2 particles [44,45].

5. Conclusions

For the first time, n-TiO_2 was functionalized with a RAFT agent, followed by living grafting from polymerization using acrylic acid as the monomer, with resultant TiO_2/PAA hybrid materials being synthesized. The RAFT agent, 2-{[(butylsulfanyl)carbonothioyl]sulfanyl}propanoic acid, was shown to be both functionalization and living polymerization agents. FTIR analysis and organic phase/water phase partitioning studies provided the evidence of the functionalization of n-TiO_2 by the RAFT agent, while GPC results of cleaved polymer after various reaction times showed that the polymerization was still living, even after the RAFT agent was coordinated to n-TiO_2. Electron microscopy images revealed the growth of the ''graft-from'' polymers around n-TiO_2, and the nanofillers were well separated and distributed in the polymer matrix. This research demonstrates that living polymerization initialized from functional groups on TiO_2 surfaces is promising to synthesize hybrid materials with an excellent dispersion of the nanofillers in the matrix.

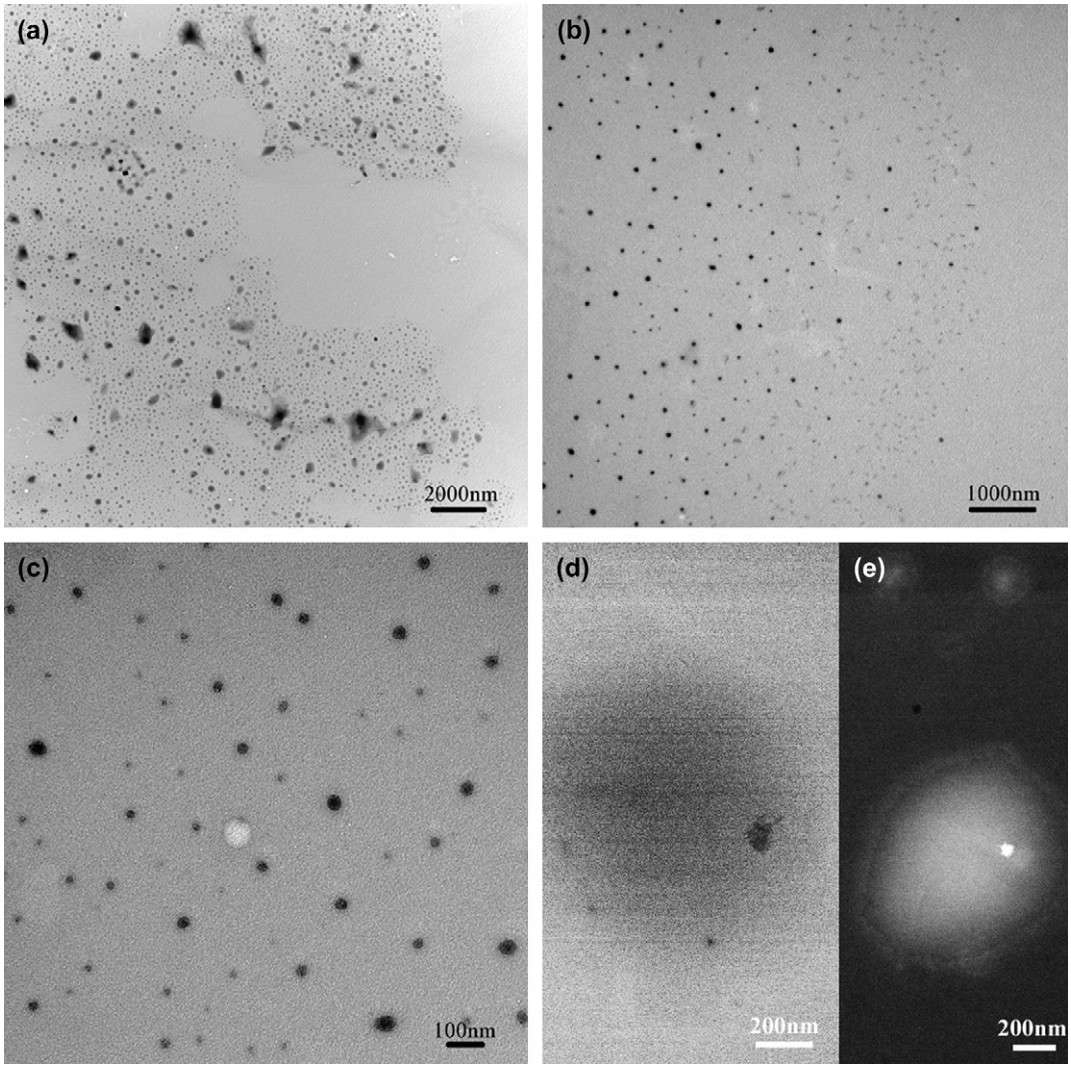

Fig. 9. TEM of the n-TiO_2/PAA at different magnification (a–c); and STEM of n-TiO_2/PAA at high magnification with bright and dark field (d–e).

Acknowledgements

We would like to thank Ronald Smith of the Department of Biology of UWO for TEM analysis, Becky Howard of Surface Science Western for FTIR analysis, William Xu and Brian Dennis for GPC analysis, Mohammad Rahbari for SEM/EDX analysis and Ilya Gourevich for TEM analysis at the University of Toronto. This work was financially supported by the Canadian Natural Science and Engineering Research Council (NSERC), the Materials and Manufacturing Ontario Emerging Materials program (MMO-EMK), and the Canadian Foundation for Innovation (CFI).

References

[1] Lecerf N, Mathur S, Shen H, Veith M, Hüfner S. Scr Mater 2001; 44:2157.
[2] Kunitake N, Fujikawa S. Aust J Chem 2003;56:1001.
[3] Lee TW, Park OO, Yoon J, Kim JJ. Adv Mater 2001;13:211.
[4] McEuen PL, Bockrath M, Cobden DH, Lu JG. Microelectron Eng 1999;47(4):417.
[5] Wypych F, Satyanarayana KG. J Colloid Interface Sci 2005; 285(2):532.
[6] Lu M-D, Yang S-M. Synth Met 2005;154(1–3):73.
[7] Teo BK, Li CP, Sun XH, Wong NB, Lee ST. Inorg Chem 2003; 42(21):6723.
[8] Petrella A, Tamborra M, Curri ML, Cosma P, Striccoli M, Cozzoli PD, et al. J Phys Chem B 2005;109(4):1554.
[9] Kocher M, Daubler TK, Harth E, Scherf U, Gugel A, Neher D. Appl Phys Lett 1998;72(6):650.
[10] Zan L, Tian L, Liu Z, Peng Z. Appl Catal A 2004;264(2):237.
[11] Bisquert J, Cahen D, Hodes G, Ruhle S, Zaban A. J Phys Chem B 2003;108(24):8106.
[12] Tokuhisa H, Hammond PT. Adv Funct Mater 2003;13(11):831.
[13] Jordan J, Jacob KI, Tannenbaum R, Sharaf MA, Jasiuk I. Mater Sci Eng 2005;A393(1–2):1.
[14] Xia H, Wang Q. Chem Mater 2002;14(5):2158.
[15] Wang Q, Xia H, Zhang C. J Appl Polym Sci 2001;80(9):1478.
[16] Xia H, Wang Q. J Appl Polym Sci 2003;87(11):1811.
[17] Rong MZ, Zhang MQ, Zheng YX, Zeng HM, Walter R, Friedrich K. Polymer 2001;42(1):167.
[18] Xie S, Zhang S, Wang F. J Appl Polym Sci 2004;94(3):1018.
[19] Jin K, Faust R. Macromol Sci Part A 2003;40(10):991–1008.
[20] Zajac R, Chakrabarti AI. Phys Rev E 1995;52(6-B):6536–49.
[21] Li C, Benicewicz BC. Macromolecules 2005;38(14):5929.
[22] Husseman M, Malmstrom EE, McNamara M, Mate M, Mecerreyes D, Benoit DG, et al. Macromolecules 1999;32:1424.
[23] Werne TV, Patten TE. J Am Chem Soc 2001;123:7497.
[24] Pyun J, Jia S, Kowalewski T, Patterson GD, Matyjaszewski K. Macromolecules 2003;36(14):5094.
[25] Carrot G, Rutot-Houze D, Pottier A, Degee P, Hilborn J, Dubois P. Macromolecules 2002;35:8400.
[26] Ohno K, Esfarjani K, Kawazoe Y. Computational materials science: from ab initio to Monte Carlo methods. Berlin; New York: Springer; 1999.
[27] Carrot G, Diamanti S, Manuszak M, Charleux B, Vairon JP. J Polym Sci Part A Polym Chem 2001;39:4294.
[28] Ejaz M, Yamamoto S, Ohno K, Tsujii Y, Fukuda T. Macromolecules 1998;31:5934.
[29] Kong H, Gao C, Yan D. Macromolecules 2004;37(11):4022.
[30] Baum M, Brittain WJ. Macromolecules 2002;35(3):610.
[31] Cui J, Wang W, You Y, Liu C, Wang P. Polymer 2004;45(26):8717.
[32] Vana P, Davis TP, Barner-Kowolik C. Macromol Theor Simul 2002; 11:823.
[33] Rotzinger FP, Kesselman-Truttmann JM, Hug SJ, Shklover V, Gratzel M. J Phys Chem B 2004;108(16):5004.
[34] Khaled SM, Sui R, Charpentier PA, Rizkalla AS. Langmuir 2007; 23(7):3988.
[35] Ferguson CJ, Hughes RJ, Pham BTT, Hawkett BS, Gilbert RG, Serelis AK, et al. Macromolecules 2002;35(25):9243.
[36] Chieffari J, Chong YK, Ercole F, Krstina J, Jeffery J, Le T, et al. Macromolecules 1998;31:5559.
[37] Ferguson CJ, Hughes RJ, Nguyen D, Pham BTT, Gilbert RG, Serelis AK, et al. Macromolecules 2005;38(6):2191.
[38] Miquelard-Garnier G, Demoures S, Creton C, Hourdet D. Macromolecules 2006;39(23):8128.
[39] Ladaviere C, Dorr N, Claverie JP. Macromolecules 2001;34:5370.
[40] Moad G, Rizzardo E, Thang SH. Aus J Chem 2005;58:379.
[41] Sui R, Rizkalla AS, Charpentier PA. J Phys Chem B 2006; 110(33):16212.
[42] Deacon GB, Phillips RJ. Coord Chem Rev 1980;33:227.
[43] Nakamoto K. Infrared and Raman spectra of inorganic and coordination compounds. New York: Wiley-Interscience Publication; 1997.
[44] Heijman SGJ, Stein HN. Langmuir 1995;11(2):422.
[45] Loiseau J, Doerr N, Suau JM, Egraz JB, Llauro MF, Ladaviere C, et al. Macromolecules 2003;36:3066.